Acta Mechanica 135, 113 – 126 (1999)

ACTA MECHANICA

The effect of the slip boundary condition on the flow of fluids in a channel

I. J. Rao and **K. R. Rajagopal,** College Station, Texas

(Received May 5, 1998)

Summary. The assumption that a liquid adheres to a solid boundary ("no-slip" boundary condition) is one of the central tenets of the Navier-Stokes theory. However, there are situations wherein this assumption does not hold. In this paper we investigate the consequences of slip at the wall on the flow of a linearly viscous fluid in a channel. Usually, the slip is assumed to depend on the shear stress at the wall. However, a number of experiments suggests that the slip velocity also depends on the normal stress. Thus, we investigate the flow of a linearly viscous fluid when the slip depends on both the shear stress and the normal stress. In regions where the slip velocity depends strongly on the normal stress, the flow field in a channel is not fully developed and rectilinear flow is not possible. Also, it is shown that, in general, traditional methods such as the Mooney method cannot be used for calculating the slip velocity.

1 Introduction

The "no-slip" boundary condition is one of the cornerstones on which the mechanics of the linearly viscous liquid is built. In his original paper, Navier [1] had proposed a slip boundary condition wherein the slip velocity depended linearly on the shear stress. Helmholtz and Pitrowski [2] introduced the notion of the "coefficient of slip" (Gleitungskoeffizient) for the slip occurring adjacent to a wall. Kundt and Warburg [3] studied the damping of a vibrating disk in a gas and found that the coefficient of slip was inversely proportional to the pressure. They also studied [4] the flow of air and hydrogen in glass tubes and again found that the coefficient of slip was inversely proportional to the pressure. Later, Maxwell [5] derived an expression for the slip of a gas next to a solid surface. A detailed discussion of the early work in this area can be found in Kennard [6].

Soon after formulating the Navier-Stokes equations, Stokes [7] considered the no-slip boundary condition but rejected it except possibly for small fluid velocities. However, in the following years as experimental evidence mounted in favor of the no-slip boundary condition for a large class of flows, and it became widely accepted for most liquid flows. An interesting account of the acceptance of the no-slip boundary condition can be found in the article by Day [8]. While this assumption has proved to be highly successful for a great variety of flow conditions, it has been found to be inadequate in certain situations: the mechanics of thin films, problems involving multiple interfaces and the flow of rarefied fluids are but a few of the examples that immediately come to mind.

The "no-slip" boundary condition is also widely used for flows involving non-Newtonian fluids past solid boundaries. However, it has been found that a large class of polymeric materials slip or stick-slip on solid boundaries. For instance, when polymeric melts flow due to an applied pressure gradient, there is a sudden increase in the throughput at a critical

pressure gradient. This phenomenon is referred to as "spurt" (Denn [9], Vinogradov et al. [10], Petrie and Denn [11]). The onset of "spurt" has been observed to coincide with the occurrence of "slip", and thus "slip" has been attributed as the cause of spurt. However, other rationale such as a non-monotonic relationship between the shear stress and shear rate (see Kolkka et al. [12], McLeish and Ball [13], Malkus et al. [14], [15], Rao and Rajagopal [16], Rao [17]) has also been advanced towards explaining the phenomenon of spurt. Other phenomena such as the "sharkskin" effect observed during oscillatory flows of constant piston speed rheometers (Hatzikiriakos and Dealy [18]) might also call into question the appropriateness of the "no-slip" boundary condition for that problem.

Considerable amount of exerimental work has been carried out to determine the nature of the slip that takes place at solid boundaries. A discussion of previous work concerning this issue of slip can be found in Petrie and Denn [11]. A taxidermy of some of the various models for slip that have been used is provided in the Appendix.

One of the early studies of the slip at the wall was undertaken by Mooney [19] who observed that the flow curves (shear stress versus nominal shear rate) of certain fluids varied with the radius of the capillary, when the stress exceeded a certain value. He inferred from this that slip was taking place at the wall and introduced an approximate methodology to calculate the slip velocity. This technique known as the Mooney technique is still widely used to measure the slip velocity. Slip has been inferred using a number of different methods. A number of workers (Hatzikiriakos and Dealy [20], [21], Ramamurthy [22]) have used the Mooney technique to estimate slip. Hot-film probes have been used (Kraynik and Schowalter [23], Lim and Schowalter [24], Atwood and Schowalter [25]) to measure the wall slip. More recent experiments (Migler et al. [26], [27]) have measured slip at the interface using an evanescent wave fluorescence technique. This technique can measure slip in a zone within about $0.1\mu m$ off the solid surface.

The slip velocity depends strongly on the shear stress, and hence most constitutive equations developed for slip assume that it depends only on the shear stress. However, it seems plausible, based on our experience from friction problems in classical physics that the mean normal stress would have an impact on the slip and this is in fact the case. The effects of normal stress on slip have been investigated in the early experiments carried out on capillary rheometers by Vinogradov and Ivanova [28]. In these experiments extrudate distortion was suppressed at elevated pressures and this was inferred to be due to a decrease in the slip velocity with increasing pressure. In more recent experiments, White et al. [29] studied the flow of elastomers in a rotational viscometer. They found that the slip velocity decreases with pressure and that above a certain pressure the slip velocity became independent of pressure. Hatzikiaros and Dealy [21] used a modified Mooney technique to determine the form of the slip equation and its dependence on normal stress and shear stress. They observed that the traditional Mooney technique for determining the slip velocity works only if the fluid is slipping by the same amount at each location in the capillary, i.e. if the flow is fully developed. If the slip velocity depends on the normal stress this condition is not satisfied, and hence the Mooney technique gives erroneous results. A consequence of this is that the data from capillary rheometers and sliding plate rheometers for slip velocity obtained using the traditional Mooney technique are inconsistent. Person and Denn [30] have carried out a much simplified one-dimensional analysis for the flow of power law fluids in a channel with a slip boundary condition that includes dependence on the pressure.

Numerical computations of the full partial differential equations incorporating constitutive equations for slip have not been fully explored. However, incorporating slip at the wall has led to a possible explanation for an interesting class of problems, a few of which are

discussed below. Georgiou and Crochet [31] with the aim of modeling the oscillations observed in constant piston speed rheometers and other extruding devices carried out computations for a compressible viscous fluid flowing through a channel with slip at the wall. In this computation the constitutive equation for slip was chosen to have a non-monotone relationship with the shear stress. By using a compressible fluid and a non-monotone constitutive equation for the slip, they were able to model the self-sustaining oscillations observed in the experiments. Sillman and Scriven [32] have carried out a computational study of the steady discharge of a Navier-Stokes fluid out of a channel. They showed that incorporating slip on the solid surface near the exit alleviates the stress singularity at the contact line. Torres et al., [33] have modeled the bicomponent coextrusion process in a square channel. In this problem the assumption of a no-slip boundary condition gives poor results as the contact line cannot move. They use a number of slip boundary conditions which suppose that the slip velocity depends on the shear stress. The numerical results of the simulations using the slip boundary condition were found to be consistent with experimental observations. Given the numerous problems in which slip seems to be critical in determining the characteristics of the flow, it seems reasonable to investigate the effect of slip in a systematic manner, and this analysis is meant to be a part of such a study.

Much of the research involving slip presumes that the slip velocity depends on the shear stress. In this paper we study the effect of including normal stresses in addition to the shear stresses in the description of the slip that occurs during the flow in a channel. We feel that before studying complicated non-Newtonian models it is useful to study the incompressible Navier-Stokes fluid under more general boundary conditions. Three different equations for slip are used here in the computations. The first model for slip depends purely on the shear stress, the second model depends only on the normal stress, and the third model reflects the dependence of slip on both the shear and normal stresses. It is found that the solutions obtained using an equation for slip that accounts for the effect of the normal stress is qualitatively different from the solutions in which the dependence of the slip velocity on the normal stress is ignored.

2 Governing equations

The Cauchy stress tensor in an incompressible Navier-Stokes fluid is given by

$$\mathbf{T} = -p\mathbf{I} + 2\mu\mathbf{D}, \tag{1}$$

where $-p\mathbf{I}$ denotes the indeterminate part of the stress due to the constraint of incompressibility, $\mathbf{D}$ is the symmetric part of the velocity gradient, i.e.

$$\mathbf{D} = \frac{1}{2}[\mathbf{L} + \mathbf{L}^T], \qquad \mathbf{L} = \operatorname{grad} \mathbf{v}, \tag{2}$$

and μ is the viscosity. As the fluid is incompressible, it can only undergo isochoric motions and therefore

$$\operatorname{div}(\mathbf{v}) = 0. \tag{3}$$

The balance of linear momentum, in the absence of body forces, is

$$\varrho\left(\frac{\partial \mathbf{v}}{\partial t} + [\operatorname{grad} \mathbf{v}]\,\mathbf{v}\right) = -\operatorname{grad}(p) + \mu\nabla^2\mathbf{v}. \tag{4}$$

In deriving (4) we have made use of (1). For the purposes of illustration, we shall consider plane flows. We now introduce the following non-dimensionalization:

$$\mathbf{v}^* = \frac{\mathbf{v}}{U}, \qquad \mathbf{x}^* = \frac{\mathbf{x}}{W}, \qquad t^* = \frac{t}{W/U}, \qquad p^* = \frac{p}{\varrho U^2}, \tag{5}$$

where W denotes the channel width and U denotes a characteristic velocity. In a two dimensional Cartesian coordinate system, the conservation of mass and balance of linear momentum in the non-dimensional form reduce to (dropping the '*' for clarity):

$$\frac{\partial u}{\partial x} + \frac{\partial v}{\partial y} = 0, \tag{6}$$

$$\frac{\partial u}{\partial t} + u\frac{\partial u}{\partial x} + v\frac{\partial u}{\partial y} = -\frac{\partial p}{\partial x} + \frac{1}{\mathrm{Re}}\left(\frac{\partial^2 u}{\partial x^2} + \frac{\partial^2 u}{\partial y^2}\right), \tag{7}$$

$$\frac{\partial v}{\partial t} + u\frac{\partial v}{\partial x} + v\frac{\partial v}{\partial y} = -\frac{\partial p}{\partial y} + \frac{1}{\mathrm{Re}}\left(\frac{\partial^2 v}{\partial x^2} + \frac{\partial^2 v}{\partial y^2}\right). \tag{8}$$

In Eqs. (6)–(8), u is the non-dimensional velocity in the x direction, v is the non-dimensional velocity in the y direction, p is the indeterminate part of the stress due to the constraint of incompressibility (which in the case of a Navier-Stokes fluid is the same as the pressure), and Re is the Reynolds number $\left(\mathrm{Re} = \frac{\varrho UW}{\mu}\right)$.

3 Relations for slip

We assume that the fluid is capable of slip, and its value depends on the extent of the normal and shear stresses at the wall, i.e. the slip velocity is a function of the shear and the normal stress at the wall:

$$u_s = f(\tau_w, \sigma_w). \tag{9}$$

For the flow of an incompressible Newtonian fluid through a channel, the shear stress at the wall is given by

$$\tau_w = \mu\left(\frac{\partial u}{\partial y} + \frac{\partial v}{\partial x}\right)\Big|_w, \tag{10}$$

and the normal stress at the wall is given by

$$\sigma_w = -p + 2\mu\frac{\partial v}{\partial y}\Big|_w, \tag{11}$$

where the suffix w implies the value at the wall. In a pressure driven flow, as the pressure drops along the direction of flow, we can expect the slip to change along the flow direction. The experiments indicate (see White et al. [29]) that the slip velocity is independent of the pressure at sufficiently high pressures; however, at lower pressures the slip velocity depends on the pressure. This presents a problem in specifying the correct boundary conditions for the numerical simulation since the exit boundary conditions cannot be accurately prescribed, as the flow is not fully developed. In order to know the correct boundary conditions, the downstream conditions after the fluid exits the channel would have to be determined in conjunction with the upstream flow. This would significantly complicate the numerical simulation. Here,

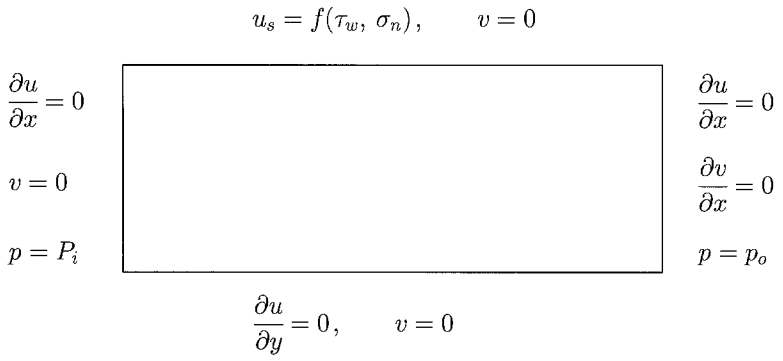

Fig. 1. Geometry and boundary conditions for the problem

we are primarily interested in gleaning a better understanding of the effect of slip on the flow in a channel, hence we will consider a simplified boundary condition at the exit as shown in Fig. 1.

There are very few experiments that attempt to quantify the pressure dependence of slip, and there is no reliable data available to generate a constitutive equation for the slip velocity taking into account both the shear and normal stresses. A number of researchers have developed slip theories (see Appendix). Since there is no agreement in the literature regarding the nature of the constitutive equation, in this study we will try to determine the differences in the solutions obtained for three boundary conditions, viz. when the slip velocity depends on the shear stress alone, when the slip velocity depends only on the normal stress and when it depends on both shear and normal stresses. For the case when the slip velocity depends solely on the shear stress, the solution of the problem is straightforward, as the flow in a long channel can now be assumed to be fully developed. A common form for the slip equation as a function of the shear stress obtained by fitting data is (cf. [20], [22], [37]–[39]):

$$\begin{aligned} u_s &= 0 \qquad \text{if} \quad \tau_w < \tau_{cr}, \\ u_s &= a(\tau_w)^m \quad \text{if} \quad \tau_w \geq \tau_{cr}, \end{aligned} \tag{12}$$

where a and m are constants, τ_w is the shear stress at the wall, and τ_{cr} the critical shear stress below which the fluid does not slip at the wall.

For the case when the slip velocity depends on the normal stress, the constitutive equation for slip is chosen so that it has a realistic dependence on the normal stress and can yield solutions consistent with the exit boundary conditions. Based on experimental evidence (see [29]), at high values of normal stresses the slip velocity is assumed to be independent of the normal stresses. Also at high values of normal stresses the slip velocity can either be zero or be non-zero; i.e. the slip velocity takes on an asymptotic value at high values of the normal stress. As the normal stress decreases it is assumed that the slip velocity increases. This also seems to be reasonable from our experience regarding problems involving friction in classical mechanics. With these two factors in mind the following slip equation will be used:

$$\begin{aligned} u_s &= u_1 \qquad \text{if} \quad \sigma_w < \sigma_0, \\ u_s &= \frac{u_1 + u_h}{2} + \frac{u_1 - u_h}{2} \sin\left(\frac{\sigma_w - \sigma_0}{\sigma_1 - \sigma_0}\,\pi + \frac{\pi}{2}\right) \qquad \text{if} \quad \sigma_0 \leq \sigma_w \leq \sigma_1, \\ u_s &= u_h \qquad \text{if} \quad \sigma_w > \sigma_1. \end{aligned} \tag{13}$$

Here σ_1 is the normal stress above which slip does not depend on the normal stress, σ_0 is the normal stress below which the slip velocity does not depend on the normal stress, u_s is the slip velocity, σ_w is the normal stress at the wall, u_h and u_1 are the limiting values of slip velocity for high and low values of the normal stress, respectively. This equation is qualitatively similar to experimental observations (White et al. [29]) for moderate to large values of the normal stress.

When the slip velocity depends on both the shear and normal stresses, we use an equation for the slip, which depends on the ratio of the shear stress to the normal stress $\left(\alpha = \frac{\tau_w}{\sigma_n}\right)$. When the value of α is large, the fluid slips and when the value of α is small the fluid does not slip, i.e. for a fixed value of shear stress larger values of normal stresses impede slip. The exact form of the equation for slip that will be used is:

$$
\begin{aligned}
&u_s = u_1 \qquad \text{if} \quad \alpha < \alpha_0\,, \\
&u_s = \frac{u_1 + u_h}{2} + \frac{u_1 - u_h}{2} \sin\left(\frac{\alpha - \alpha_0}{\alpha_1 - \alpha_0}\,\pi + \frac{\pi}{2}\right) \qquad \text{if} \quad \alpha_0 \le \alpha \le \alpha_1\,, \\
&u_s = u_h \qquad \text{if} \quad \alpha > \alpha_1\,, \qquad \text{where} \quad u_h > u_1\,.
\end{aligned}
\tag{14}
$$

Here, we assume that for both large and small values of α the slip velocity is independent of α, however the independent values at the large and small limits are different. For intermediate values of α, the slip velocity varies with α in a manner consistent with the lower and higher limits.

Various other dependencies for the slip velocity on the shear and normal stresses could be assumed. We shall not do so here but rest content with the cases discussed above as they between them cover qualitatively some of the possibilities that we could encounter in a real flow situation.

4 Flow domain and boundary conditions

The geometry of the flow domain along with the boundary conditions is provided in Fig. 1. The problem is solved only in the top half of the channel because we seek solutions having symmetry about the centerline. The velocity is assumed to be fully developed at the inlet, and pressures are prescribed at the inlet and at the outlet. The velocity gradients in the main flow direction are set to zero at the exit. The lower boundary conditions are prescribed according to the symmetry of the problem. At the top (next to the wall) the boundary condition is that the vertical velocity is zero (impermeable wall) and the horizontal velocity is determined by the equation for slip. All the solutions were obtained on a channel of length $L = 4$ and width $W = 1$.

5 Numerical scheme

The coupled partial differential equations governing the problem (Eqs. (6)–(8)) are solved using a finite volume method. The problem was solved on a staggered grid with the velocities defined at the boundaries of each control volume and the pressure at the center of the control volume. These equations were solved using a modification of the projection method introduced by Chorin [34]; the details on this variant of the projection method can be found in the text by Fletcher [35]. In flows involving convective terms, special techniques have to be used to discretize the convective terms so as to minimize the error due to "numerical diffusion".

Techniques developed for capturing sharp gradients in the flows of compressible fluids have been very effective in the flows of incompressible fluids. A flux corrected transport algorithm developed by Van-Leer [36] was used to discretize the convective terms. In the projection method at each time step a Poisson equation has to be solved for the pressure. This Poisson equation was solved using a multigrid algorithm. The integration in time is done using an explicit scheme till a steady state is achieved. As an initial condition the fluid was assumed to be stationary. At each step, the boundary conditions on the velocities have to be updated as they depend on the flow field. The slip velocity at the boundary was increased incrementally to speed up the convergence to the steady state. The results were solved on the largest grid for which grid independence of the solution was verified. A 64×16 grid was found to be sufficient for this problem.

6 Results

When the problem is solved using an equation for slip that does not incorporate the normal stresses, fully developed flow is observed along the length of the channel. If the shear stress at the wall is greater than the critical shear stress τ_{cr}, the flow slips at the wall and conversely if the shear stress is not large enough, then the classical Poiseuille solution with no-slip is observed. The steady state solution is easily obtained and is shown in Fig. 2. Also, since the flow is assumed to be fully developed the pressure gradient is linear along the length of the channel, and there is no flow in the vertical direction. However, when the slip velocity is assumed to depend on the normal stress, the slip velocity varies along the length of the channel and hence the x and y components of the velocities also vary along the length of the channel.

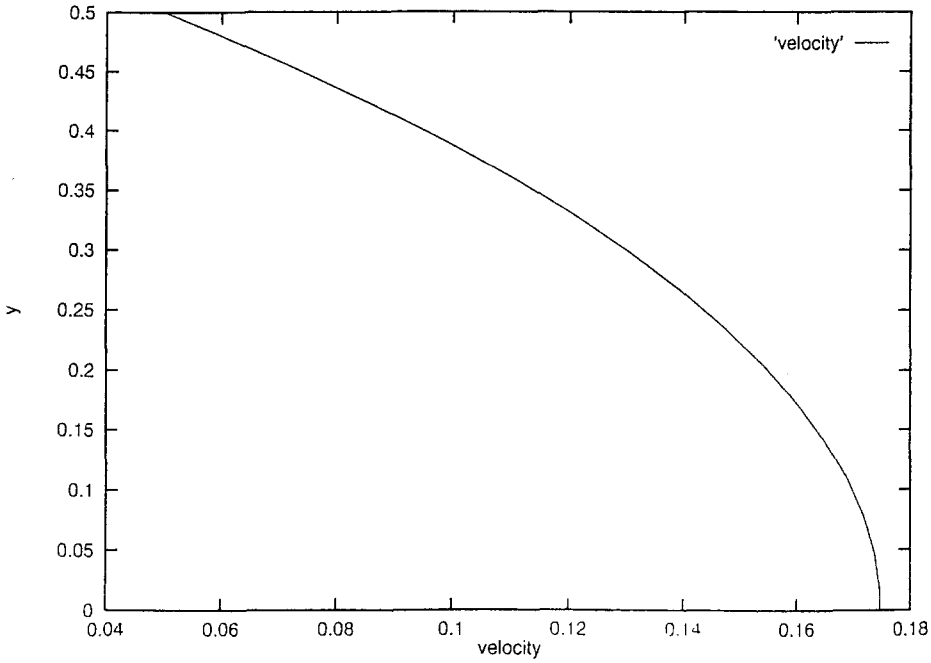

Fig. 2. Velocity profile with slip when the slip velocity depends only on the shear stress $\left(\mathrm{Re} = 1, \frac{\partial p}{\partial x} = 1, u_s = 0.05\right)$

This behavior is very different from the velocity profiles obtained by using equations for the slip that imply that slip does not depend on the normal stress.

For the case when the slip velocity depends only on the normal stress, the velocity at the inlet is assumed to be fully developed and the slip equation is chosen such that the asymptotic value of the slip velocity at high values of normal stress is zero (i.e. $u_h = 0$ in Eq. (15)). At the inlet, the axial velocity is parabolic and the vertical component of velocity is zero. As the fluid flows down the channel, the pressure drops and consequently the normal stress at the wall also drops. When the normal stress drops below the critical value σ_1, slip is initiated at the wall and increases as the normal stresses decrease. The horizontal velocities at the inlet and outlet of the channel are shown in Fig. 3. We notice that the velocity profiles at the inlet and outlet are qualitatively different with the outlet velocity being much blunter than the one at the inlet, due to which the shear stress at the wall is greater at the inlet than at the outlet. When the fluid starts slipping at the wall with different velocities at different axial locations the vertical component of the velocity can no longer remain zero if conservation of mass is to be satisfied. Figure 4 shows the vertical component of the velocities at different axial locations, and we note that it is much smaller than the horizontal component. As the pressure drops further, the normal stress drops below σ_0 and the slip velocity becomes independent of the normal stress, i.e., the vertical component of the velocity again goes to zero and the axial velocity tends to a new fully developed state. The pressure at the centerline of the channel is plotted in Fig. 5. The pressure gradient is linear near the inlet and the exit of the channel where the flow is fully developed, but with different slopes and near the center where redistribution of the velocity profile is taking place the pressure gradient is not linear. The dashed lines in Fig. 5 show the pressure gradients at the inlet and outlet, the difference between which

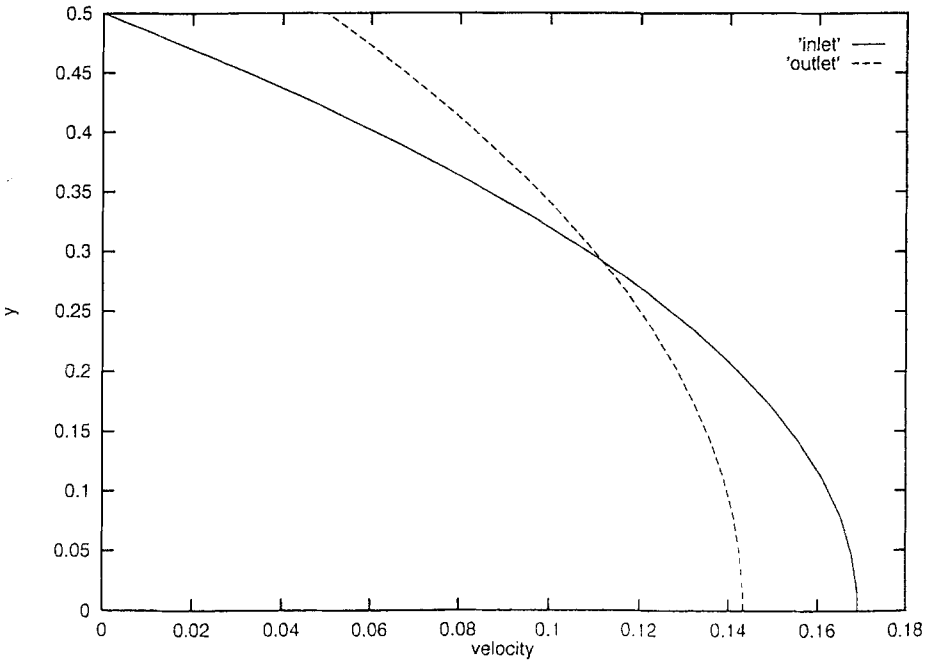

Fig. 3. Axial velocity profile at the inlet and exit of the channel when the slip velocity depends on the normal stress (Re = 1, $P_i = 5$, $P_0 = 1$, $u_1 = 0.05$, $u_h = 0.0$, $\sigma_0 = 1.75$, $\sigma_1 = 4.0$)

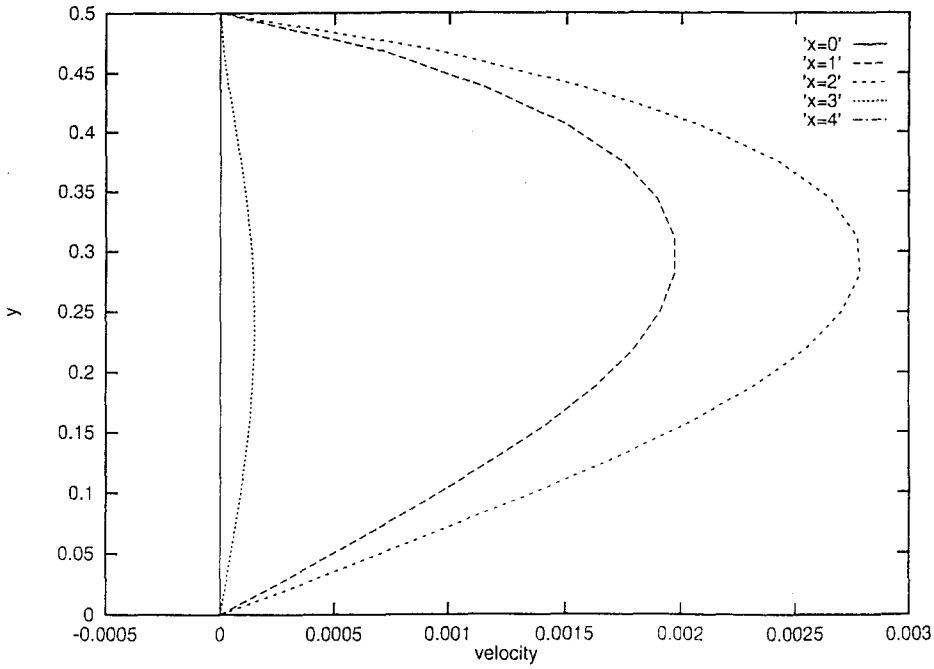

Fig. 4. Vertical velocity profile at different axial locations when the slip velocity depends on the normal stress (Re = 1, $P_i = 5$, $P_0 = 1$, $u_1 = 0.05$, $u_h = 0.0$, $\sigma_0 = 1.75$, $\sigma_1 = 4.0$)

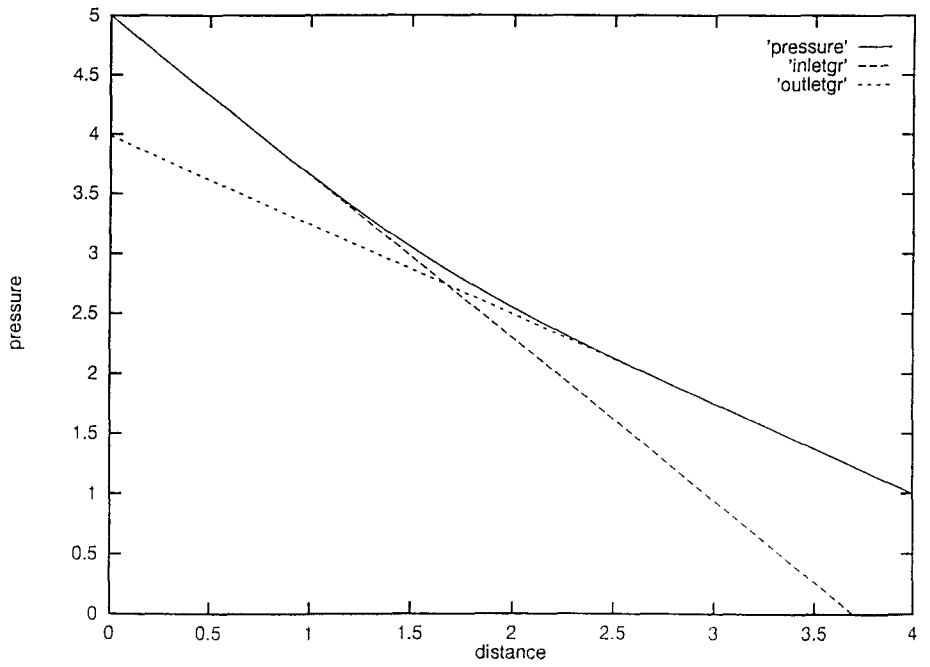

Fig. 5. The variation of the centerline pressure along the length of the channel when the slip velocity depends on the normal stress (Re = 1, $P_i = 5$, $P_0 = 1$, $u_1 = 0.05$, $u_h = 0.0$, $\sigma_0 = 1.75$, $\sigma_1 = 4.0$)

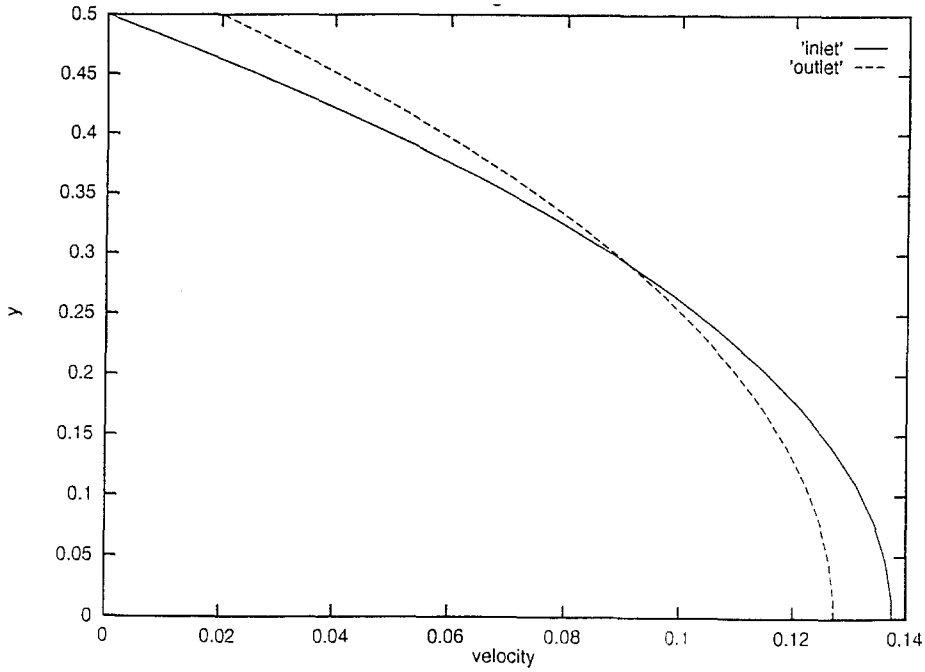

Fig. 6. Axial velocity profile at the inlet and exit of the channel when the slip velocity depends on the shear and normal stresses (Re = 1, $P_i = 5$, $P_0 = 1$, $u_1 = 0.0$, $u_h = 0.02$, $\alpha_0 = 0.12$, $\alpha_1 = 0.22$)

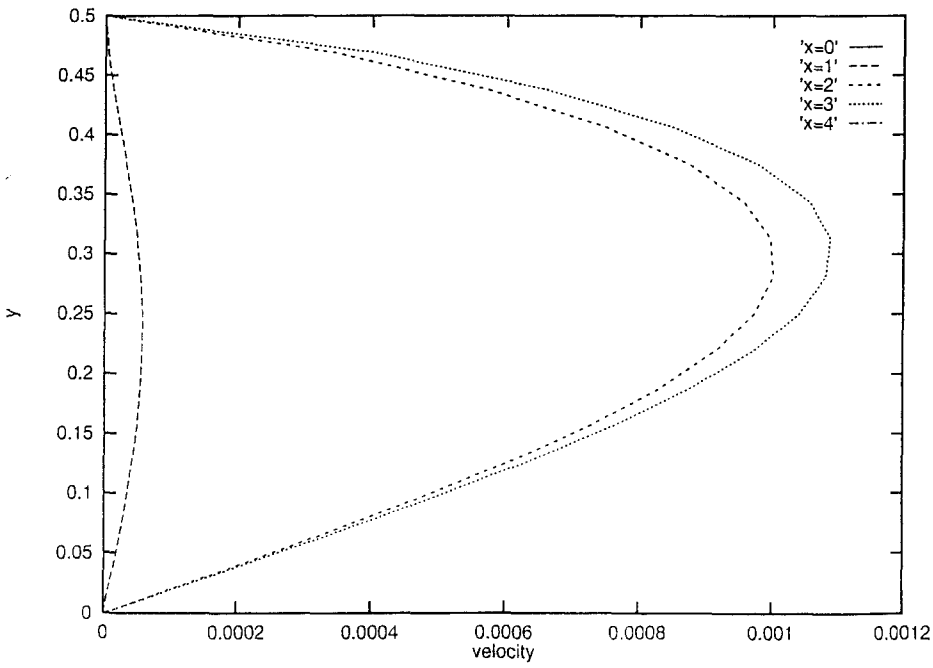

Fig. 7. Vertical velocity profile at different axial locations when the slip velocity depends on the shear and normal stresses (Re = 1, $P_i = 5$, $P_0 = 1$, $u_1 = 0.0$, $u_h = 0.02$, $\alpha_0 = 0.12$, $\alpha_1 = 0.22$)

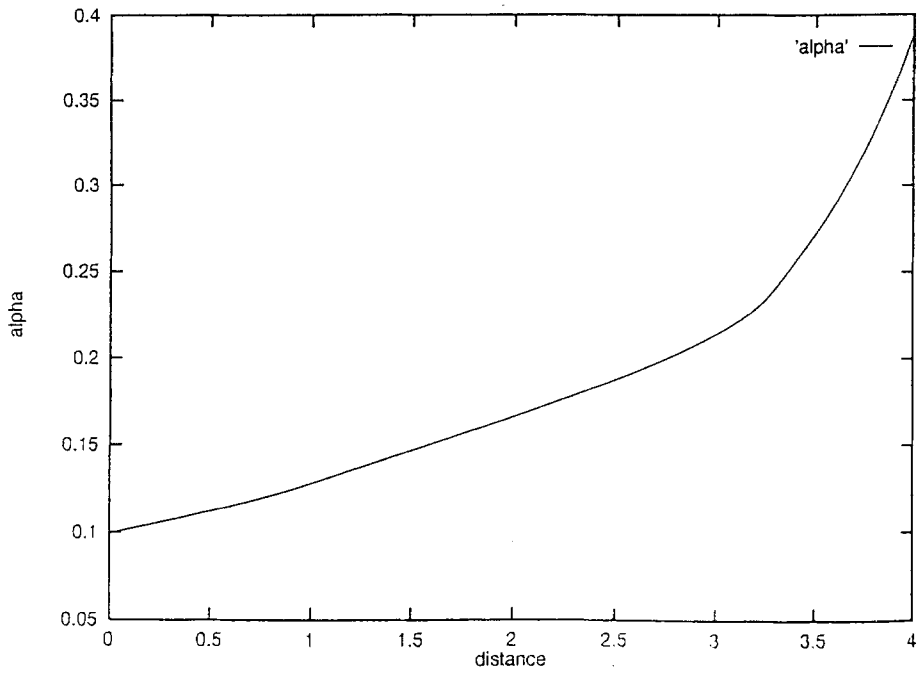

Fig. 8. The variation of α along the length of the channel when the slip velocity depends on the shear and normal stresses (Re = 1, $P_i = 5$, $P_0 = 1$, $u_1 = 0.0$, $u_h = 0.02$, $\alpha_0 = 0.12$, $\alpha_1 = 0.22$)

is significant. The pressure gradient at the inlet is greater than the pressure gradient at the outlet, and this is consistent with the observation that the shear stress at the inlet is greater than the shear stress at the outlet. When both the effects of normal and shear stresses are incorporated into the equation governing slip, the solutions obtained are qualitatively similar to the case when the slip velocity depends only on the normal stress. When the fluid enters the channel, the pressure is high and therefore the value of α is low, and thus at the inlet the fluid is assumed to have zero velocity at the wall (i.e., $u_1 = 0$ in Eq. (16)). As the fluid flows down the channel the pressure drops, and consequently the value of α increases till it is larger than α_0 and slip takes place at the boundary. As the fluid flows further down the channel the value of α increases till it exceeds α_1 and the slip velocity becomes constant and independent of α. Figure 6 shows the inlet and outlet velocity components in the x direction. The velocity profile at the inlet is fully developed and parabolic with no-slip while at the exit the velocity profile is fully developed and parabolic with slip. When the fluid starts slipping, the velocity in the y direction cannot remain zero. The velocity components in the vertical direction are plotted at different axial locations in Fig. 7. The vertical velocities at the inlet and outlet are zero. It follows once again that the pressure does not vary linearly along the pipe. The value of α along the length of the channel is shown in Fig. 8.

7 Conclusions

When the slip at the wall depends on the normal stresses, the velocity field is qualitatively different from that for the case when it depends purely on the shear stress. When the slip velocity depends only on the shear stress, the velocity components depend only on the y coordinate, and the solution is very similar to a classical Poiseuille solution but with non-zero

velocites at the boundaries. However, if the slip velocity does depend on the normal stress, the velocity field depends both on the x and y co-ordinates, and there are two components to the velocity field. Another important difference is that the pressure gradient is no longer linear along the channel. Due to these differences in the flow fields, traditional methods like the Mooney technique, which presuppose a fully developed flow with a linear pressure gradient are ineffective for calculating the slip velocities.

Appendix

A number of models have been advanced for describing the slip that occurs at solid boundaries. We shall document some of them here. The earliest boundary condition for slip was proposed by Navier [1] in his original paper on linearly viscous fluids. It was a linear relationship between the slip velocity and the shear stress at the wall,

$$u_s = -\lambda \tau_w , \tag{A.1}$$

where λ is a constant.

Later Mooney [19] suggested that the slip velocity depended more generally on the shear stress at the wall and introduced an experimental technique for evaluating this relationship. This condition has been generalized in a variety of different ways in the subsequent literature and it has the form:

$$u_s = f(\tau_w) . \tag{A.2}$$

A number of authors (Chauffoureaux et al. [37], Lau and Schowalter [38], Ramamurthy [22], Hatzikiaros and Dealy [20], Cohen and Metzner [39]) have fitted a power-law equation to relate the slip velocity to the shear stress at the wall, and the equation has the form:

$$u_s = A[f(\tau_w)]^m , \tag{A.3}$$

where A and m are constants. The idea of a yield stress below which there is no slip is easily incorporated into such an equation.

Georgiou and Crochet [31] use a non-monotone relationship between the slip velocity and shear stress. Their equation for the boundary condition has the form:

$$\tau_w = \alpha_1 \left(1 + \frac{\alpha_2}{1 + \alpha_3 (u_s)^2} \right) u_s , \tag{A.4}$$

where α_1, α_2 and α_3 constants.

The equation for describing the slip developed empirically by Hatzikiriakos and Dealy [21] to account for the effect of normal stresses has the form:

$$u_s = \xi f_1(T) \left(1 - c_2 \tanh \left[\frac{\left(E + c_3 \dfrac{\sigma_n}{\tau_w} \right)}{RT} \right] \right) (\tau_w)^m , \tag{A.5}$$

where ξ, c_2, c_3 and E are constants, R is the universal gas constant, T is the temperature and f_1 is a function which includes the effects of temperature.

Person and Denn [30] use an equation for the slip having the form:

$$u_s = a(\tau_w)^m \exp(-\beta_s p) , \tag{A.6}$$

where a, m and β_s are constants and p is the pressure.

A number of mathematicians have used various slip boundary conditions. We provide a few examples below.

Serrin [40] used the following boundary condition:

$$\begin{aligned} &|\tau_w| < k|\sigma_n| \Rightarrow \mathbf{u}_s = 0\,, \\ &|\tau_w| > |\sigma_n| \Rightarrow \mathbf{u}_s = -\lambda\left(1 - k\frac{|\sigma_n|}{|\tau_w|}\right)\sigma_n\,. \end{aligned} \tag{A.7}$$

Consiglieri [41] used the following form for the slip:

$$\begin{aligned} &|\tau_w| < k|\sigma_n| \Rightarrow \mathbf{u}_s = 0\,, \\ &|\tau_w| = k|\sigma_n| \Rightarrow \mathbf{u}_s = -\lambda\tau_w\,. \end{aligned} \tag{A.8}$$

Fujita [42] used the following slip boundary condition:

$$\begin{aligned} &|\tau_w| \leq g\,, \\ &\mathbf{u}_s = 0 \qquad \text{or} \qquad |\mathbf{u}_s|\tau_w = -g\mathbf{u}_s\,. \end{aligned} \tag{A.9}$$

Note: In the above boundary conditions $\mathbf{u}_s$, τ_w and σ_n are the slip velocity, tangential shear stress and the normal stress respectively, all measured at the wall. All three are vectors. The constants k, λ and g are positive scalars.

Acknowledgement

Support from the National Science Foundation is gratefully acknowledged.

References

[1] Navier, C. L. M. H.: Sur les lois du mouvement des fluides. Mem. Acad. R. Sci. Inst. Fr. **6,** 389–440 (1827).
[2] Helmholtz, H., Pitrowski, G. v.: Über Reibung tropfbarer Flüssigkeiten. Wissenschaftliche Abhandlungen **I,** 172–222, Leipzig 1882.
[3] Maxwell, J. C.: On stresses in rarified gases arising from inequalities in temperature. In: The scientific papers of James Clerk Maxwell (Niven, W. D., ed.) Volume **II,** pp. 681–712. Cambridge: Cambridge University Press 1890.
[4] Kundt, A., Warburg, E.: Über Reibung und Wärmeleitung verdünnter Gase. Ann. Phys. Chem. **155,** 337–365 (1875).
[5] Kundt, A., Warburg, E.: Über specifische Wärme des Quecksilbergases. Ann. Phys. Chem. **157,** 353–364 (1876).
[6] Kennard, E. H.: Kinetic theory of gases. New York: McGraw Hill 1938.
[7] Stokes, C. G.: Mathematical and physical papers, vol. 1. Cambridge: Cambridge University Press 1880.
[8] Day, M. A.: The no-slip boundary condition in fluid mechanics. Erkenntnis **33,** 285–296 (1990).
[9] Denn, M. M.: Issues in viscoelastic fluid mechanics. Ann. Rev. Fluid Mech. **22,** 13–34 (1990).
[10] Vinogradov, G. V., Malkin, A. Ya., Yanovskii, Yu. G., Borisenkova, E. K., Yarlykov, B. V., Brezhnaya, G. V.: Viscoelastic properties and flow of narrow distribution polybutadienes and polyisopropenes. J. Polymer Sci. Part A-2, **10,** 1061–1084 (1972).
[11] Petrie, C. J. S., Denn, M. M.: Instabilites in polymer processing. AIChE J. **22,** 209–236 (1976).
[12] Kolkka, R. W., Malkus, D. S., Hansen, M. G., Ierly, G. R., Worthing, R. A.: Spurt phenomena for the Johnson-Segalman fluid and related models. J. Non-Newtonian Fluid Mech. **29,** 303–335 (1988).
[13] McLeish, T. C. B., Ball, R. C.: A molecular approach to the spurt effect in polymer melt flow. J. Polymer Sci., Part B, **24,** 1735–1745 (1986).
[14] Malkus, D. S., Nohel, J. A., Plohr B. J.: Dynamics of shear flow of a non-Newtonian fluid. J. Comp. Phys. **87,** 464–487 (1990).

[15] Malkus, D. S., Nohel, J. A., Plohr, B. J.: Analysis of a new phenomenon in shear flow of non-Newtonian fluids. SIAM J. Appl. Math. **51,** 899–929 (1991).
[16] Rao, I. J., Rajagopal, K. R.: Some simple flows of a Johnson-Segalman fluid. Acta Mech. **132,** 209–219 (1999).
[17] Rao, I. J.: Flow of a Johnson-Segalman fluid between rotating co-axial cylinders with and without suction. Int. Non-Linear Mech. **34,** 63–70 (1999).
[18] Hatzikiriakos, S. G., Dealy, J. M.: Role of slip and fracture in the oscillatory flow of HDPE in a capillary. J. Rheol. **36,** 845–884 (1992).
[19] Mooney, M.: Explicit formulae for slip and fluidity. J. Rheol. **2,** 210–222 (1931).
[20] Hatzikiriakos, S. G., Dealy, J. M.: Wall slip of molten high density polyethylene I. Sliding plate rheometer studies. J. Rheol. **35,** 497–523 (1991).
[21] Hatzikiriakos, S. G., Dealy, J. M.: Wall slip of molten high density polyethylene's II. Capillary rheometer studies. J. Rheol. **36,** 703–741 (1992).
[22] Ramamurthy, A. V.: Wall slip in viscous fluids and influence of material construction. J. Rheol. **30,** 337–357 (1986).
[23] Kraynik, A. M., Schowalter, W. R.: Slip at the wall and extrudate roughness with aqueous solutions of polyvinyl alcohol and sodium borate. J. Rheol. **25,** 95–114 (1981).
[24] Lim, F. J., Schowalter, W. R.: Wall slip of narrow molecular weight distribution polybutadienes. J. Rheol. **33,** 1359–1382 (1989).
[25] Atwood, B. T., Schowalter, W. R.: Measurement of slip at the wall during the flow of high density polyethylene through a rectangular conduit. Rheol. Acta **28,** 134–146 (1989).
[26] Migler, K. B., Hervet, H., Leger, L.: Slip transition of a polymer melt under shear stress. Phys. Rev. Lett. **70,** 287–290 (1993).
[27] Migler, K. B., Massey, G., Hervet, H., Leger, L.: The slip transition at the polymer-solid interface. J. Phys. Condens. Matter **6,** A301–304 (1994).
[28] Vinogradov, G. V., Ivanova, L. I.: Wall slippage and elastic turbulence of polymers in the rubbery state. Rheol. Acta **7,** 243–254 (1968).
[29] White, J. L., Han, M. H., Nakajima, N., Brzoskowski, R.: The influence of materials of construction on biconical rotor and considerations of slippage. J. Rheol. **35,** 167–189 (1991).
[30] Person, T. J., Denn, M. M.: The effect of die materials and pressure-dependent slip on the extrusion of linear low-density polyethylene. J. Rheol. **41,** 249–265 (1997).
[31] Georgiou, C. G., Crochet, M. J.: Compressible viscous flow in slits with slip at the wall. J. Rheol. **38,** 639–654 (1994).
[32] Sillman, W. J., Scriven, L. E.: Separating flow near a static contact line: slip at a wall and shape of a free surface. J. Comp. Phys. **34,** 287–313 (1980).
[33] Torres, A., Hrymak, A. N., Vlachopoulos, J., Dooley, J., Hilton, B. T.: Boundary conditions for contact lines in coextrusion flows. Rheol. Acta **35,** 513–525 (1993).
[34] Chorin, A. J.: Numerical solution of the Navier-Stokes equations. Math. Comput. **22,** 745–762 (1968).
[35] Fletcher, C. A. J.: Computational techniques for fluid dynamics, vol. II. Berlin Heidelberg New York Tokyo: Springer 1991.
[36] Van Leer, B.: Flux-vector splitting for the Euler equations. Lecture Notes in Physics, vol. 70, 507–512 (1982).
[37] Chauffoureaux, J. C., Dehennau, C., Van Rijckevorsel, J.: Flow and thermal instability of rigid PVC. J. Rheol. **23,** 1–24 (1979).
[38] Lau, H. C., Schowalter, W. C.: A model for adhesive failure of viscoelastic fluids during flow. J. Rheol. **30,** 193–206 (1986).
[39] Cohen, Y., Metzner, A. B.: Apparent slip flow of polymer solutions. J. Rheol. **29,** 67–102 (1985).
[40] Serrin, J.: Mathematical principles of classical fluid mechanics. In: Encyclopedia of Physics, vol. III/1 (Flügge, S., Truesdell, C., eds.). Berlin: Springer 1959.
[41] Consiglieri, L.: Stationary solutions for a Bingham flow with nonlocal friction. In: Mathematical topics in fluid mechanics (Rodrigues, J., Sequeira, A., eds.). Pitman Research Notes in Mathematics, **274**. Essex: Longman Scientific and Technical 1992.
[42] Fujita, H.: A mathematical analysis of motions of viscous incompressible fluids under leak or slip boundary conditions. Surikaisekikenenkyusho Kokyuroko **734,** 123–142 (1990).

Author's address: I. J. Rao and K. R. Rajagopal, Department of Mechanical Engineering, Texas A & M University, College Station, TX 77863, U.S.A.